Serial noninvasive photoacoustic imaging of neovascularization in tumor angiogenesis

R.I. Siphanto[1]*, K.K. Thumma[2]*, R.G.M. Kolkman[2], T.G. van Leeuwen[2], F.F.M. de Mul[2], J.W. van Neck[1], L.N.A. van Adrichem[1] and W. Steenbergen[2]

1 Erasmus MC – University Medical Center Rotterdam, Department of Plastic and Reconstructive Surgery, PO Box 1738, NL-3000 DR Rotterdam, The Netherlands
2 University of Twente, Faculty of Science and Technology, Biophysical Engineering Group, PO Box 217, NL-7500 AE Enschede, The Netherlands
w.steenbergen@utwente.nl

**These authors contributed equally to this work*

Abstract: We present photoacoustic images of tumor neovascularization obtained over a 10-day period after subcutaneous inoculation of pancreatic tumor cells in a rat. The images were obtained from ultrasound generated by absorption in hemoglobin of short laser pulses at a wavelength of 1064 nm. The ultrasound signals were measured in reflection mode using a single scanning piezodetector, and images were reconstructed with a weighted delay-and-sum algorithm. Three-dimensional data visualize the development and quantify the extent of individual blood vessels around the growing tumor, blood concentration changes inside the tumor and growth in depth of the neovascularized region.

OCIS codes: (170.5120) Photoacoustic imaging; (170.0110) Imaging systems; (170.4580) Optical diagnostics for medicine; (300.1030) Absorption.

References and links

1. J. Folkman, "Angiogenesis in cancer, vascular, rheumatoid and other disease," Nat. Med. **1**, 27-31 (1995).
2. J. Folkman, "New perspectives in clinical oncology from angiogenesis research," Eur. J. Cancer **32A**, 2534-2539 (1996).
3. J. Hasan, R. Byers, and G.C. Jayson, "Intra-tumoral microvessel density in human solid tumors," Br. J. Cancer **86**, 1566-1577 (2002).
4. M.W. Dewhirst, B. Klitzman, R.D. Braun, D.M. Brizel, Z.A. Haroon, and T.W. Secomb, "Review of methods used to study oxygen transport at the microcirculatory level," Int. J. Cancer **90**, 237-255 (2000).
5. M.D. Menger, M.W. Laschke, and B Vollmar, "Viewing the microcirculation through the window: some twenty years experience with the hamster dorsal skinfold chamber," Eur. Surg. Res. **34**, 83-91 (2002).
6. M.V. Knopp, H. von Tengg-Kobligk, and P.L. Choyke, "Functional magnetic resonance imaging in oncology for diagnosis and therapy monitoring," Mol. Cancer Ther. **2**, 419-426 (2003).
7. M. Krix, F. Kiessling, S. Vosseler, N. Farhan, M.M. Mueller, P. Bohlen, N.E. Fusenig, and S. Delorme, "Sensitive noninvasive monitoring of tumor perfusion during antiangiogenic therapy by intermittent bolus-contrast power Doppler sonography," Cancer Res. **63**, 8264-8270 (2003).
8. H. Anderson, P. Price, M. Blomley, M.O. Leach, and P Workman, "Measuring changes in human tumor vasculature in response to therapy using functional imaging techniques," Br. J. Cancer **85**, 1085-1093 (2001).
9. T.L. Collier, R. Lecomte, T.J. McCarthy, S. Meikle, T.J. Ruth, F. Scopinaro, A. Signore, H. VanBrocklin, C. Van de Wiele, and R.N. Waterhouse, "Assessment of cancer-associated biomarkers by positron emission tomography: advances and challenges," Dis. Markers **18**, 211-247 (2002).
10. C.G.A. Hoelen, F.F.M. de Mul, R. Pongers, and A. Dekker, "Three-dimensional photoacoustic imaging of blood vessels in tissue," Opt. Lett. **23**, 648-650 (1998).
11. X.D. Wang, Y.J. Pang, G. Ku G, X.Y. Xie, Stoica G, and L.H.V. Wang, "Noninvasive laser-induced photoacoustic tomography for structural and functional in vivo imaging of the brain," Nat. Biotechnol. **21**, 803-806 (2003).
12. A.A. Karabutov, V.A. Andreev, B.A. Bell, R.D. Fleming, Z. Gatalica, M. Motamedi, E.V. Savateeva, H. Singh, S.V. Solomatin, S.L. Thomsen, M. Henrichs, and A.A. Oraevsky, "Optoacoustic images of early cancer in forward and backward modes," in *Hybrid and Novel Imaging and New Optical Instrumentation for Biomedical Applications*, A. Boccara and A.A. Oraevsky; eds., Proc. SPIE **4434**, 13-27 (2001).

#5641 - $15.00 US Received 3 November 2004; revised 17 December 2004; accepted 21 December 2004

13. A.A. Oraevsky, A.A. Karabutov, S.V. Solomatin, E.V. Savateeva, V.A. Andreev, Z. Gatalica, H. Singh, R.D. Fleming, "Laser optoacoustic imaging of breast cancer in vivo," in *Biomedical Optoacoustics II*, Proc. SPIE **4256,** 6-15 (2001).
14. R.A. Kruger, K.D. Miller, H.E. Reynolds, W.L. Kiser, D.R. Reinecke, and G.A. Kruger, "Breast cancer in vivo: contrast enhancement with thermoacoustic CT at 434 MHz-feasibility study," Radiology **216**, 279-283 (2000).
15. C.G.A. Hoelen, and F.F.M. de Mul, "Image reconstruction for photoacoustic scanning of tissue structures," Appl. Opt. **39**, 5872-5883 (2000).
16. M.C. Pilatou, N.J. Voogd, F.F.M. de Mul, W. Steenbergen, and L.N.A. van Adrichem, "Analysis of three-dimensional photoacoustic imaging of a vascular tree in vitro," Rev. Sci. Instrum. **74**, 4495-4499 (2003).
17. C.G.H. Hoelen, A. Dekker, and F.F.M.de Mul, "Detection of photoacoustic transients originating from microstructures in optically diffuse media such as biological tissue", IEEE Trans. Ultrason. Ferroelectr. Freq. Control **48**, 37-47 (2001).
18. R.A.Kruger, W.L. Kiser, D.R. Reinecke, and G.A. Kruger, "Thermoacoustic computed tomography using a conventional linear transducer array," Med. Phys. **30**, 856-860 (2003).
19. C.G.A. Hoelen, and F.F.M. de Mul, "A new theoretical approach to photoacoustic signal generation," J. Acoust. Soc. Am. **106**, 695-706 (1999).
20. S. Achilefu, R.B. Dorshow, J.E. Bugaj, and R. Rajagopalan, "Novel receptor-targeted fluorescent contrast agents for in vivo tumor imaging,". Invest. Radiol. **35**, 479-485 (2000).
21. P. Carmeliet, and R.K. Jain, "Angiogenesis in cancer and other diseases," Nature **407**, 249-257, (2000).
22. S. Ramanujan, G.C. Koenig, T.P. Padera, B.R. Stoll and R.K. Jain, "Local imbalance of proangiogenic and antiangiogenic factors: a potential mechanism of focal necrosis and dormancy in tumors," Cancer Res. **60**, 1442-1448 (2000).
23. G.L. Semenza, "Hypoxia-inducible factor 1: master regulator of O2 homeostasis," Curr. Opin. Genet. Dev. **8**, 588-594 (1998).
24. S.J. van Belle, and V. Cocquyt, "Impact of haemoglobin levels on the outcome of cancers treated with chemotherapy," Crit. Rev. Oncol. Hematol. **47**, 1-11 (2003).
25. X.D. Wang, G. Ku, M.A. Wegiel, D.J. Bornhop, G. Stoica, L.H.V. Wang, "Noninvasive photoacoustic angiography of animal brains in vivo with near-infrared light and an optical contrast agent," Opt. Lett. **29**, 730-732 (2004).

1. Introduction

Knowledge of the important role of vascularization in tumor development [1, 2] has led to recognition of the prognostic value of tumor angiogenesis, and to proposition of anti-angiogenic therapies [3-6]. Tools for monitoring such therapies should be noninvasive, and give quantitative information on the developing vascular bed associated with in situ tumors. Histologic microvessel density counts [3] and intravital microscopy [4, 5], lack some of these features. Noninvasive methods like magnetic resonance imaging6, ultrasound7, and positron emission tomography [8, 9], are being introduced for neovascularization assessment. However, these often involve contrast agents. A potential noninvasive technique using natural contrast is photoacoustic imaging [10, 11]. Here, we present images of tumor neovascularization obtained over a 10-day period after subcutaneous inoculation of pancreatic tumor cells in a rat. Three-dimensional data visualize the development and quantify the extent of individual blood vessels around the growing tumor, blood concentration changes inside the tumor and growth in depth of the neovascularized region.

Photoacoustics refers to the conversion of light into sound by optical absorption. In biomedical photoacoustic imaging, pulsed laser light applied e.g. percutaneously, is predominantly absorbed by hemoglobin in blood. This causes a small local rise in temperature, restricted dilatation of the red blood cells and subsequent elevation of the local pressure. Consequently ultrasonic waves are generated, which, when measured in a sufficient number of locations at the tissue surface, can be used to reconstruct the position of blood vessels in three dimensions [10].

The technique has already been used to visualize optical inhomogenities with sub-millimeter sizes in phantoms and biological tissue [10, 12], while others have demonstrated photoacoustic mammography [13, 14].

This study was designed to evaluate the potential of in vivo photoacoustic imaging of the developing vasculature from the early stage of tumor growth.

#5641 - $15.00 US Received 3 November 2004; revised 17 December 2004; accepted 21 December 2004

2. Materials and methods

2.1 Photoacoustic sytem, scanning procedure

As light source, an Nd:YAG laser (LS 2139, Lotis TII, Russia) was used. The laser emitted infrared light at 1064 nm in 14 nanosecond pulses with a repetition rate of 50 Hertz.

The photoacoustic sensor consisted of a disk shaped piezoelectric detector with a diameter of 200 µm and a detection bandwidth of 65 MHz, allowing high-resolution three-dimensional visualization of vasculature [15, 16]. The detector was covered by a 9 µm thick layer of polyvinylidene difluoride (PVdF) film, which served as sensing material [17]. Two optical fibers with a core diameter of 600 µm that were integrated in the detector were used for light delivery. A digitizer (DC265, Acqiris, Switzerland) received the signals at sampling rate of 500 Msamples/s and transferred the digitized signal to a computer for subsequent data processing. During scanning the output energy of the fibers was maintained at approximately 2.3 mJ/pulse. The distance between the detector and the sample surface was ~5 mm in all experiments. This resulted in an irradiated area on the sample surface of 0.05 cm². Thus, the energy density used in all experiments was below 50 mJ/cm^2. In each detection point, the recorded signal was the average of the signals of 16 laser pulses. The size of the scanned region was 15x15 mm^2, with a distance between the detection points of 0.15 mm. Hence, a measurement grid of 100x100 points was adopted.

In contrast to studies where circular or cylindrical scanning modes were adopted [11, 18], here the measurements were carried out in reflection mode, implying that illumination and ultrasonic detection are on the same side.

2.2 Image reconstruction, scaling and representation

A weighted delay and sum focused beam forming algorithm was used for reconstruction of the three-dimensional acoustic source distribution [15, 19]. In this algorithm, the image value S^f in tissue voxel f is determined as

$$S^f = \frac{\sum_{i=1}^{N} w_i^f s_i(t + \delta_i^f)}{\sum_{i=1}^{N} w_i^f} \qquad (1)$$

with $s_i(t)$ the acoustic signal recorded in detector position *i*, w_i^f the weighing factor taking into account the angular sensitivity of detector i for signals generated in voxel *f*, and the distance between these points, δ_i^f the arrival time delay at detector position *i* after the laser pulse of the acoustic wave generated in voxel *f*. In each voxel, the image value is taken as the root mean square of the back-projected acoustic signal in that voxel. Images are presented as maximum intensity projections (MIP) viewed in z-direction and slices in the xz-plane. In the MIPs each pixel value is the maximum intensity over all voxels in the stack below the corresponding pixel.

2.3 Animal model

The experimental procedures in this study were approved by the committee on animal welfare of the Erasmus Medical Center Rotterdam. The well-characterized rat tumor model CA20948 was used [20]. A male Lewis rat weighing 250 g was used for the experiments. The hind limb was chosen because it is minimally influenced by the animal's breathing excursions. The hind limb of the animal was shaven and chemically depilated. Subsequently, a suspension of 6x10^6 pancreatic tumor cells was subcutaneously injected in the right hind limb. An area of approximately 1.5x1.5 cm^2 around the inoculation site was defined by a marker in order to locate the same spot for serial scanning. After tumor inoculation the animal was allowed to recover before starting the photoacoustic scanning procedure.

#5641 - $15.00 US Received 3 November 2004; revised 17 December 2004; accepted 21 December 2004

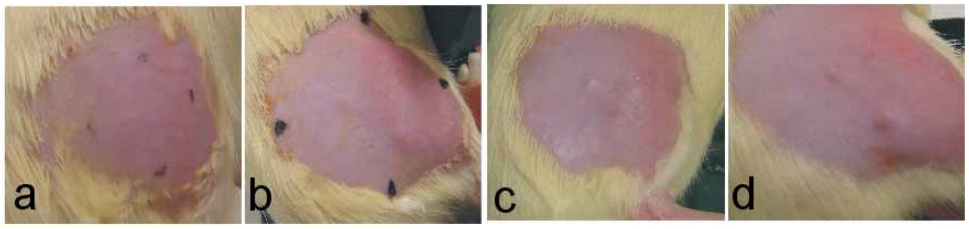

Fig. 1. Serial photographs of the tumor inoculation site on the hind limb of the animal, on day 3 (a), day 7 (b), day 8 (c) and day 10 (d).

Photoacoustic scanning was performed on day 3, 7, 8 and 10, with the day of inoculation counted as day 1. Morphologic evaluation of the tumor was performed on a daily basis. Tumor growth was estimated in time by two-dimensional measurements with calipers and presented as surface area.

Photoacoustic scanning was done under gaseous isoflurane anaesthesia (Rhodia Organique Fine Ltd., Avonmouth Bristol, UK). To prevent hypothermia the animal was placed on an electric heating blanket and the animal received an injection of saline solution every hour to maintain blood pressure. The hind limb was covered by sufficient amounts of ultrasound gel (Sonogel, Germany) to provide an acoustic coupling medium for the acoustic pressure waves.

3. Results

3.1 External appearance of tumor site

As for the visual appearance of the tumors, on day 3 no sign of tumor growth could be seen. From day 7, the external appearance of the inoculation site (Fig. 1) showed the progressive growth of the tumor. On day 7 a small nodular mass of approximately 3x5 mm^2 could be palpated on the skin. By day 8 the tumor began to develop a visible subcutaneous purple mass at the inoculation area. On day 10 the tumor mass was quite elevated and reached a surface area of approximately 240 mm^2 estimated by calipers. The boundaries of the tumor exceeded the scanning area (225 mm^2), therefore only part of the tumor was scanned.

3.2 Photoacoustic images

Three-dimensional data reconstructed from the acoustic signals are presented as maximum intensity projections (MIP) viewed in the z-direction (Fig. 2) and slices in the xz-plane (Fig. 3). The color scaling in all projection images refers to the same range of absolute values. Hence, amplitude differences throughout the days, as displayed by the images, represent real changes in the signal strength.

No blood vessels can be observed (Fig. 2) in the photoacoustic image recorded on day 3. The series of images reveal a major increase in photoacoustic response in the period between day 3 and day 7. On day 7, three blood vessels can be observed in the upper part of the image and one on the lower part, which are leading to or from a central structure, suggesting a tumor mass surrounded by developing vessels. On day 8, signal intensity has further increased. Two of the vessels visible on day 7 are still present in the upper right half corner, while the images of the two other vessels are more faded. Also, the amplitude in the part where the blood vessels connect is enlarged. It is more difficult to correlate the image of day 10 with the previous ones. Signal amplitude has not increased, but the structure of the image has changed.

The development in the z-direction is presented in the form of equidistantly positioned slices in the xz-plane, with a thickness of 150 µm (Fig. 3). While the skin surface is not discernible in these slices due to the chosen color scale, it could be observed from a detailed assessment of signal values. Based on this, the skin contour has been constructed and is indicated in the slices by a thin white line. Between day 3 and day 8, the photoacoustic signal originates from a region with a thickness of 0.5-0.75 mm, extending down to 1-1.5 mm below the skin surface. Between day 8 and day 10, an increase from the depth range of the

#5641 - $15.00 US Received 3 November 2004; revised 17 December 2004; accepted 21 December 2004

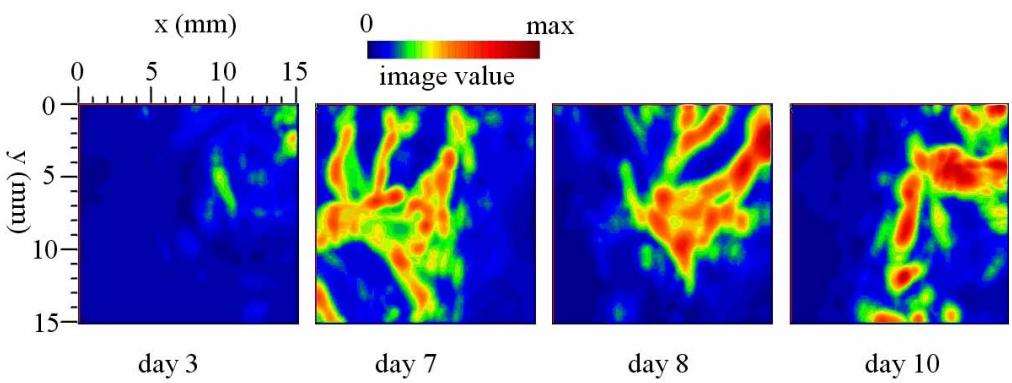

Fig. 2. Photoacoustic images: maximum intensity projections of the acoustic source strength in the xy-plane (top view on the tissue, with in each pixel the maximum value found in all voxels below that pixel) on the indicated days (tumor cells inoculated on day 1). The color scaling in all images relates to the same absolute value. Therefore the images reveal the development of the amplitude of the photoacoustic signals during the tumor growth process.

reconstructed objects is observed. On day 10 the thickness of the region that contains acoustic sources is about 1.5 mm, extending down to 2-2.5 mm below the skin contour.

There is qualitative agreement between the external appearance of the tumor site (Fig. 1) and the photoacoustic slices in the xz-plane (Fig. 3), in that in both visualizations a clear protuberance in the skin contour can be seen on day 10 which was much smaller or absent on previous days.

4. Discussion

At a wavelength of 1064 nm, the strongest absorber in the tissue studied here is oxyhemoglobin. Based on this knowledge, on the morphology of the photoacoustic images and the general experience collected on photoacoustic imaging, it is highly probable that the visualized structures are related to newly formed blood vessels.

Our images strongly suggest the formation and/or growth of blood vessels in the inoculation region between day 3 and day 7, and a growth in depth of the tissue volume contributing to the images between day 8 and day 10. The images of day 7 and 8 are morphologically related, but they do not suggest a continuous progression of vascular growth with new vessels being added to the existing network: some of the vessels visible on day 7 are not visible, or less pronounced, on day 8. The morphologic relation between day 8 and day 10 is less obvious.

The absence of progression in the photoacoustic images may be related to the chaotic and poorly regulated growth in cancer. Abnormal branching of the vascular network combined with diminished expression of angiogenic factors in certain areas of the tumor results in less angiogenesis This leads to the formation of hypoxic and necrotic regions, two well-known features of tumors [21, 22]. For the used wavelength of 1064 nm, light absorption by hemoglobin is reduced in hypoxic regions, while in necrotic regions no hemoglobin is present. As a consequence of hypoxia and necrosis, photoacoustically silent regions may be created inside the tumor, while at this wavelength the lower oxygen saturation in the veins will reduce their photoacoustic contrast.

Since in this study a single detector was used rather than an array, mechanical step scanning was performed, leading to a measurement time of 0.54 seconds per point, and a total scan duration of 1.5-2 hours. Long scan durations may have led to image blurring and reduction of the imaging resolution due to subject movements. With the use of a single scanning transducer, a less dense grid than adopted in this investigation will lead to some

#5641 - $15.00 US Received 3 November 2004; revised 17 December 2004; accepted 21 December 2004

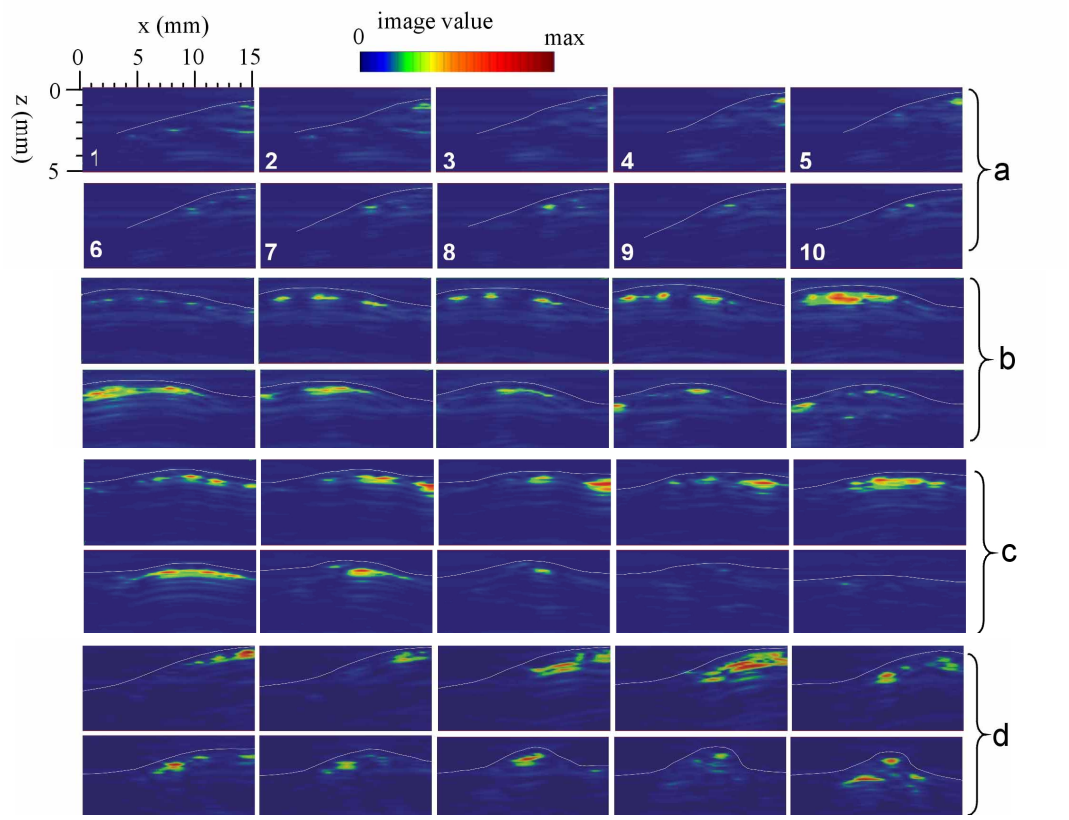

Fig. 3. Depth development of blood vessels. Slices of 150 micrometers thickness in the xz-plane, evenly distributed over the next ranges of y-positions: Fig. a (day 3): 0<y<6.75 mm; Fig. b, c, d (day 7-10): 0<y<15 mm; Images for day 3 are numbered 1..10 in the order of increasing y-position with image 1 at y=0 mm, with identical order for the other days. The thin white line indicates the skin contour.

reduction of the scanning time. For the used transducer of 200 µm diameter, a grid distance of 200 µm instead of 150 µm will be allowed without loss of image quality. This will reduce the scanning time with a factor 0.6. The largest reduction of the scanning time will be realized by using an array of simultaneously sampled acoustic detectors and a laser with a higher pulse repetition rate. More rapid imaging not only improves the quality of the images, but also will allow for scanning larger tissue areas, and will facilitate the procedure for probe alignment and definition of the tissue area to be scanned. Furthermore, a short acquisition time will allow for imaging at a better time resolution, which will yield a more continuous recording of changes in the tumor vasculature. The necessity of taking images at shorter time intervals is underlined by the morphologic differences between the images of day 7, 8 and 10.

Because photoacoustics is non-invasive, tumor neovascularization can be monitored without sacrificing the animal, which enables serial measurements in the same animals. In particular this feature makes photoacoustics a promising new tool in tumor angiogenesis research. Furthermore, non-invasive assessment of the extent of tumor vasculature may become of importance in clinical evaluation of the tumor and monitoring therapy based on angiogenesis inhibition. The measurement strategy followed in our study is not restricted to superficial tumors and can therefore be applied to study tumors *in situ* rather than implanted under the skin. Furthermore, our reflection mode approach can also be applied clinically, once the measurement time is reduced to an acceptable level.

The current study was performed with a single wavelength and using the endogenous contrast provided by the blood vessels. When performed spectroscopically, photoacoustics

#5641 - $15.00 US Received 3 November 2004; revised 17 December 2004; accepted 21 December 2004

accommodates for the local determination of hemoglobin oxygenation levels. Hypoxia is regarded as an important trigger of events leading to expression of angiogenic growth factors [23]. Also, evidence is accumulating that hypoxia is correlated with poor clinical outcome, suggesting that low levels of hemoglobin negatively influence treatment outcome [24]. Furthermore, the use of contrast agents, either non-specific such as recently shown for indocyanine green polyethylene glycol in the mouse brain [25], or with specific capabilities of targeting tumor cells, may further enhance the potential of the technique for use in oncology research and for clinical purposes.

5. Conclusions

This study shows that photoacoustics is able to non-invasively monitor the development of elevated concentrations of hemoglobin in and around growing superficial tumors. Furthermore, we show the technique's ability to visualize the development of the larger arteries and veins connected to the tumor. This has been demonstrated by a series of photoacoustic images, obtained from a growing tumor implanted under the skin of a rat, over a period of 10 days, using light with a wavelength of 1064 nm, and measuring in reflection mode.

These results demonstrate the potential of the method to become a tool in tumor angiogenesis research in small animals. Further quantitative assessment of photoacoustic imaging for this application will require comparison against a reference method, for instance to determine the relation between our images and the local microvessel density (using histology), or to draw conclusions regarding necrosis and hypoxia and their effect on our images.

Spectroscopic implementation of photoacoustics may yield a more complete picture of the tumor in terms of blood oxygenation and water content. Further realization of increased imaging speed and depth will bring us closer to clinical application of the technique for tumor diagnosis and treatment monitoring.

Acknowledgments

We thank Mr. H.F. Bernard (Dept. of Nuclear Medicine) for supplying us with the tumor rats. This work was supported by the Netherlands Technology Foundation STW (grant TTN4662) and the Netherlands Foundation of Fundamental Research on Matter FOM (grant 00PMT22).

#5641 - $15.00 US Received 3 November 2004; revised 17 December 2004; accepted 21 December 2004